Static and dynamic testing on prestressed concrete slab elements with artificial bond deficiencies

J. Mahowald, S. Maas & D. Waldmann
University of Luxembourg, Faculty of Sciences, Technology and Communication, Luxembourg, Luxembourg

A. Zuerbes
Fachhochschule Bingen, Bingen, Germany

ABSTRACT: In this paper dynamic and static test procedures on industrially prestressed slab elements are presented. The aim of the tests is to provide information on the pretension force in the slabs, and therefore, on their serviceability. In order to evaluate panels with different pretension forces, the testing objects are artificially damaged by inhibiting the bond between concrete and the tendons. The conducted dynamic and static tests are unable to detect the artificial failure, as production tolerances of the slabs preponderate over the changes of the bending stiffness due to the changed pretension force. Nevertheless, the analysis of the cracking loads perfectly confirmed the reduced pretension, allowing the estimation of the pretension force of the tendons.

1 INTRODUCTION

Industrially manufactured prestressed slab elements are often used in civil engineering constructions, e.g. park decks, office and residential buildings, etc. However, a check of the pretension force after production is no more possible. Hence, for reasons of quality assurance the University of Luxembourg and the manufacturer of these slabs ECHO make research on establishing a quality test in order to verify the correct pretension force in these slabs after production. In addition, the test must be non-destructive at least for the intact slabs. In an effort, the information on the pretension force should therefore be retrieved by finding dynamic or static parameters sensitive to the pretension force in the investigated slabs.

1.1 *Description of the panels*

The investigated panels are manufactured by ECHOLUX, subsidiary of ECHO placed in Luxembourg, and are of type VSF-15-120. They are made of concrete C50/60 with a measured average compressive strength of 58.3 N/mm^2 (quality control of manufacturer). The quality of the reinforcement is St 1470/1670 and the corresponding elastic modulus 205000 N/mm^2. In the upper section of the panel 4 wires are placed with a diameter of 5 mm and in the lower section 12 wires with a diameter of 7 mm. Figure 1 shows the cross section of the prestressed concrete slabs with the reinforcement in the upper and lower part.

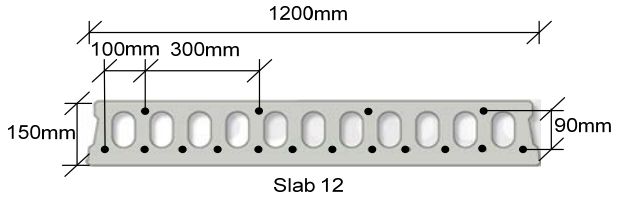

Figure 1: Cross section of the intact slab with 12 faultless tendons in the lower part.

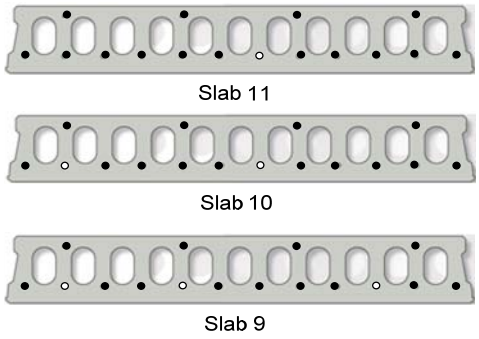

Figure 2: Cross section of the slabs with defect tendons marked in white.

Figure 3: Artificial bond deficiency of a tendon by inserting into a plastic tube.

From the manufacturer eight panels, two of each type, are provided as shown on Figure 1 and 2. The slabs are denominated by the number of intact tendons, i.e. Slab 12, Slab11, Slab10 or Slab9. The artificial failure is put into practise by a thin plastic tube inhibiting completely the bond between the steel and concrete. Figure 3 shows a picture of one laid bare tendon with tube at the end of the slab.

1.2 *Theoretical background*

The question arises, why static and dynamic tests should work on identifying pretension defects on such prestressed slabs. In theory the deformation and the eigenfrequencies of a beam depend on the bending stiffness of the material, as shown in equations (1) and (2). The bending stiffness is defined as the multiplication of the elastic modulus E by the moment of inertia I. The maximum deformation f_m of a single-span-beam due to a point charge F (to simulate our single-span-slab) is calculated according equation (1):

$$f_m = \frac{Fl^3}{48EI} \tag{1}$$

whereas l stands for the span lenght and F the point charge in the middle of the slab. Moreover, for the dynamic method, the first eigenfrequency of the same single-span-slab can be calculated as follows with M the mass per unit length:

$$f = \frac{\pi}{2l^2} \cdot \sqrt{\frac{EI}{M}} \tag{2}$$

Regarding these equations, the deflections and the eigenfrequency are independent of the pretension force concluding that static and dynamic tests inapplicable evaluating pretension defects in the slabs. However, experimental test results, shown by Saidii et al (1994) and by the University of Luxembourg (Waltering 2009), reveal the decrease of natural frequencies by increasing pretension force. Waltering presented this behaviour on a reinforced beam for different compression stresses, from 0.2 N/mm^2 to 4.8 N/mm^2 induced by a steel cable, which pretension force is increased using a hydraulic jack in longitudinal direction. Therefore, contrarily to the investigated slabs in this paper, the compression stress of the beam is increased in the same object, making the eigenfrequencies perfectly comparable according the pretension force. Here, for the investigated slabs, as four different slabs are provided, also production tolerances have to be considered.

Table 1 and Figure 4 show the first three eigenfrequencies of the gradually pretensioned concrete beam. One can clearly see that the eigenfrequencies rises with increasing compression stress. The reason is that micro-cracks in the concrete close due to higher pretension forces. This results in an increase of the bending stiffness and leads to both, the augmentation of the eigenfrequency and a minimised statical deformation under a given load.

Moreover, other former tests made at the University of Luxembourg (Mahowald et al, 2010), on a prestressed and non-prestressed concrete slab of the same type, showed also differences in eigenfrequencies: 11.75 Hz versus 11.00 Hz and in deformation: 1.73 mm versus 2.5 mm.

One can conclude that, regarding the above mentioned results, the pretension force has an impact on the apparent Youngs modulus and thus static and dynamic parameters, making these favourable for research on the quality control.

Table 1. Eigenfrequencies of a stepwise pretensioned concrete beam (Waltering 2009).

Compression stress	*mode 1-B1*	*mode 2-B2*	*mode 3-B3*
0.2 N/mm^2	18.5 Hz	51.6 Hz	97.9 Hz
1.5 N/mm^2	18.8 Hz	52.1 Hz	101.0 Hz
2.4 N/mm^2	18.9 Hz	52.5 Hz	102.5 Hz
4.8 N/mm^2	19.4 Hz	53.9 Hz	105.3 Hz

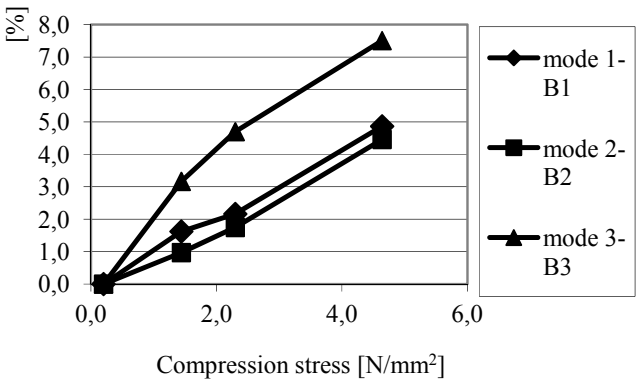

Figure 4. Percentage augmentation of the eigenfrequencies of Table 1 of the stepwise prestressed concrete beam (Waltering 2009).

2 TESTING METHODS

2.1 *Experimental setup*

For the dynamic and static testing of the slabs, three different test series are conducted. In an effort, for the first test series, the aim was to unify static and dynamic testing methods to manifest the possible use of dynamic and static parameters yielding the different pretension forces of the slabs (Viera, 2010). As the results from the first test series did not show the expected behaviour the testing procedures are modified for the second (Ries, 2010) and third test series (Tibolt, 2011) in order to improve the analysis on the investigated parameters. The static system of the first test series consists in evaluating the deflection when loading the different slab with first a steel weight of 946 kg, followed by an unbalanced mass

exciter with a weight of 578 kg, as shown on Figure 5. For the dynamic tests, only the unbalanced mass exciter is put on the slab.

Figure 5. Experimental setup for the static testing for the first test series with an unbalanced special mass exciter.

In the second test series the mass-loading was increased until a first crack occurs (varying each from 15 to 850 kg). In addition, regarding dynamic testing, the slabs are excited by an electromagnetic shaker of type TIRAvib 2.7kN (henceforth named Shaker) instead of the unbalanced mass exciter to measure the eigenfrequencies in an unloaded state. This exciter is not standing on the structure but on the floor and exciting the structure via a load-cell and a stinger.

Finally, for the third test series, the second set of slabs with the same artificial failures is measured for better visualisation and analysis of the static parameters. Here, after loading with 3 steel weights (beam blanks of 858 kg (1), 846 kg (2) and 852 kg (3), Figure 6 & Figure 7) the slabs are continuously loaded by filling water into an empty tank with a constant flow rate. Unfortunately for Slab9 a first crack occurred unexpected already after loading with the three steel weights even before putting the empty tank on.

One has to add, that for all the test series the dimension and type of bearing conditions rest the same. The span length of the slabs is 6.2 m and the loaded length is 0.9 m. Table 2 recapitulates the different characteristics of each test series.

Table 2. Summary of the different test series.

Test series	*Slab set*	*Maximum load*	*Dynamic*
First	1	1524 kg	mass exciter
Second	1	Cracking	Shaker
Third	2	Cracking*	Shaker

*(continuous loading)

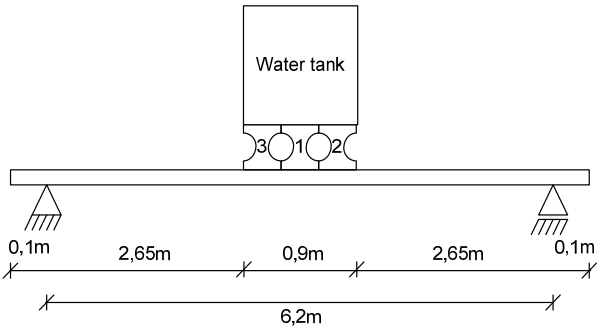

Figure 6. Sketch of the experimental setup for the static testing for the third test series with three steel weights and water tank.

Figure 7. Experimental setup for the static testing for the third test series with the three steel weights and the water tank.

2.2 *Data acquisition and test procedures*

Figure 8 shows the measurement device for the dynamic and static testing. The accelerometers for the dynamic measurements of type B393B04 from PCB Piezotronics are equally distributed over the span length with the dimensions illustrated on Figure 8 (idem for the displacement transducers).
The displacement transducers are of type HBM W1-T 100 sampled by 4 Hz. The acquisition software is Signal Express by National Instruments. The force transducers to capture the dynamic force for the unbalanced mass shaker are of type HBM U10M and for the electromagnetic shaker of type 208C03 from PCB Piezotronics. The sample rate for the dynamic tests is 1000Hz and the sweep rate 0.05 Hz/s with force amplitudes of 20, 50 and 100 N from 2 to 12 Hz for the electromagnetic shaker and 50, 75 and 100 N for the unbalanced mass exciter.

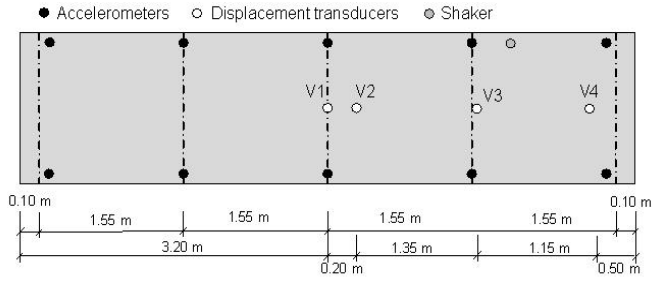

Figure 8. Experimental setup for the dynamic and static testing: in black the positions of the accelerometers, in white the positions of the displacement transducers and in grey the position of the shaker for the second and third test series.

3 TEST RESULTS

3.1 *Dynamic tests*

For the first test series, as already mentioned in the previous section, the slabs are excited by an unbalanced mass exciter with an own weight of 578kg, in an effort combining static and dynamic testing methods to evaluate the artificial reduced in pretension force. One has to add that this special exciter cannot introduce dynamic force amplitudes below 50 N into the slabs. The revealed eigenfrequencies, calculated by Mescope Software using the global polynomial method, can be seen on Table 3 for the first test series. Here, no information on the pretension force is yield from the first eigenfrequency. It seems that Slab9 and Slab11 are the stiffest ones, which is contradictory to theory, pretending that with increasing pretension force micro cracks in concrete closes, leading to higher eigenfrequencies. The major reason for the false logical order is the variation due to production tolerances in the bending stiffness, i.e. changes in the elastic modulus E or changes in the moment of inertia I, which, modified already for an example by 5%, involves changes up to 2.5% in the eigenfrequencies (Ries, 2010).

Moreover for the first test series in order to evaluate reproducible test results (difficult to achieve same bearing conditions), the essay for Slab11 is repeated twice: first by removing and putting the mass exciter again on the slab (Slab11repeated1) and second by removing the slab from the bearings and setting it again (Slab11repeated2). Already here, small changes can be recognised. Thus, concluding for the first test series one could state that the variations in the eigenfrequencies cannot be attributed exclusively to the loss in pretension forces, but also to structural and experimental differences.

Table 3. Eigenfrequencies for an excitement force of 50 N, 75 N and 100 N for the first test series loaded with 578 kg.

Eigenfrequencies EF [Hz]	*50N*	*75N*	*100N*
Slab12	5.92	5.92	5.90
Slab11	6.15	6.15	6.11
Slab11repeated1	6.14	6.14	6.11
Slab11repeated2	6.17	6.17	6.13
Slab10	6.06	6.05	6.00
Slab9	6.17	6.17	6.10

Regarding the second test series on Table 4 the same behaviour as for the first test series with the same slabs is identified. Also here Slab11 shows the highest eigenfrequencies making the dynamic parameter not adequate for retrieving information on the pretension force.

Table 4. Eigenfrequencies for an excitement force of 20 N, 50 N and 100 N for the second test series and force excitation amplitude dependency of the eigenfrequencies.

EF [Hz]	*20N*	*50N*	*100N*	$\frac{f_{100N}-f_{20N}}{f_{20N}}$
Slab12	7.85	7.81	7.73	-1.5%
Slab11	7.96	7.88	7.88	-1%
Slab10	7.91	7.83	7.84	-0.9%
Slab9	7.86	7.84	7.76	-1.3%

Table 5. Eigenfrequencies for an excitement force of 20 N, 50 N and 100 N for the third test series and force excitation amplitude dependency of the eigenfrequencies.

EF [Hz]	*20N*	*50N*	*100N*	$\frac{f_{100N}-f_{20N}}{f_{20N}}$
Slab12	8.18	8.15	8.11	-0.9%
Slab11	8.14	8.12	8.05	-1.1%
Slab10	8.12	8.09	8.06	-0.7%
Slab9	8.05	8.02	7.99	-0.7%

In contrast to the first set of slabs measured for the first and second test series, the second set of panels, i.e. the third test series, the right order of the revealed values on Table 5 is identified. Slab12 shows the highest eigenfrequency, followed by Slab11, Slab10 and Slab9. However, this correlation to the pretension force could also be a coincidence, as for the first set of panels the contrary is discovered.

Another point is the evaluation of the eigenfrequencies for the loaded slabs. Here, the experimental load should open the micro-cracks due to the additional bending stress which countervails the different normal stresses depending on the pretension force (N.B. 1 covered wire represents a reduction of 8 % of the pretension force). Therefore, the idea is to maximise the load and measure the eigenfrequencies. Tables 6 & 7 show the eigenfrequencies of the slabs without cracks formed for both sets of panels when loaded with 2449 kg and 2556 kg respectively. Regarding the values also here no trustful information is given by the results. For the first set of panels on Table 6 Slab10 seems stiffer than Slab12. In contrast, on Table 7 the eigenfrequencies for the second set of panels exhibit the right order according the pretension force, as already seen for the unloaded case. Concluding, here again the variations of concrete or the bearing conditions plays the predominant role in contrast to the changes due to the pretension force.

Table 6. Eigenfrequencies measured with a swept sine amplitude force of 20 N, 50 N and 100 N for the second test series mass-loaded with 2449 kg.

EF [Hz]	*20N*	*50N*	*100N*	$\frac{f_{100N}-f_{20N}}{f_{20N}}$
Slab12	4.16	4.18	4.16	0%
Slab11	/	/	/	
Slab10	4.17	4.17	4.17	0%
Slab9	/	/	/	

Table 7. Eigenfrequencies measured with a swept sine amplitude force of 20 N, 50 N and 100 N for the third test series mass-loaded with 2556 kg

EF [Hz]	*20N*	*50N*	*100N*	$\frac{f_{100N} - f_{20N}}{f_{20N}}$
Slab12	4.23	4.22	4.21	-0.5%
Slab11	4.21	4.20	4.18	-0.7%
Slab10	4.17	4.16	4.16	-0.2%
Slab9	/	/	/	

Furthermore, regarding the excitation force amplitude dependency of the eigenfrequencies in the last column on Tables 4, 5, 6 & 7, one observes for both sets that with increasing force, the eigenfrequencies decrease. This behaviour yields nonlinearities in the slabs. Nevertheless, no significant information of this decrease can be associated to the pretension force.

3.2 *Static tests*

For the static tests, only the deflection of transducer V1 in the middle of the slabs is presented (figure 8). Conferring to the first test series, illustrated on Table 9, the same pattern as for the dynamic testing, namely that Slab11 and Slab9 seem the stiffest ones, retrieved by the least deflection, is noticed.

Table 8. Static deformation [mm] for the first test series.

Load [kg]	*946*	*1524*	*946*	*0*
Slab12	4.50	8.05	4.92	0.28
Slab11	4.35	7.50	4.80	0.37
11repeated1	4.24	7.25	4.50	0.18
11repeated2	4.20	7.18	4.42	0.11
Slab10	4.54	7.78	4.98	0.38
Slab9	4.35	7.60	4.90	0.38

Also here changes due to the repetition of the experiment can be seen, 7.5 mm in contrast to 7.18 mm, thus 4 % differences. This reinforces the fact that variations cannot be attributed only to pretension forces, but also to structural and experimental differences.

Regarding Table 10, here for the second test series the same slabs are charged until cracking load. Slab11 shows again the least deflection for a given experimental mass, for example 7.8 mm compared to 8.4 mm, 8 mm and 8.2 mm for 1687 kg. Nevertheless with increasing load one can clearly notice that Slab12 can handle the highest weight before cracking (italic on Table 10). For Slab9 a first crack occurred already when loaded with 2601 kg, whereas for Slab10, Slab11 and Slab12, 2800 kg, respectively 3200 kg and 3300 kg is achievable before cracking.

In addition, the deflection is also in correlation with the pretension force. Slab12 shows the highest deflection with 18.2 mm, whereas for Slab11 16.5 mm, Slab10 14.6 mm and Slab9 13.6 mm is observed. Thus, one can retain that the cracking load is a trustful indicator on the pretension force. To have proof of this and to get more accurate measurement points to establish a force-deflection diagram during continuous loading, the third test series with the second set of panels was done. Unfortunately, as already mentioned, for Slab9 a crack directly occurred with the last weight. Nevertheless, regarding all the other slabs the cracking load and deflections show the same behaviour as already for first set of panels (Table11). These parameters are proper indicators on the pretension force, making the tests reproducible and applicable for a possible semi-destructive quality test.

Table 9. Static deformation [mm] for the second test series.

Load [kg]/ Deflection [mm]	*Slab 9*	*Slab 10*	*Slab 11*	*Slab 12*
0	0	0	0	0
841	4	3.9	3.8	3.9
1687	8.4	8	7.8	8.2
2601	*13.6*	/	/	/
2633		13.1	12.4	13.2
2800		*14.6*	/	/
3091			15.5	16.3
3167			16.0	16.7
3200			*16.5*	
3300				*18.2*

Table 10. Static deformation [mm] for the third test series.

Load [kg]/ Deflection [mm]	*Slab 9**	*Slab 10*	*Slab 11*	*Slab 12*
0	0	0	0	0
858	4	3.8	3.7	3.8
1704	8.3	7.9	7.6	7.7
2556		12.4	11.9	12.0
2986		*15.5*	14.8	14.6
3126			15.8	15.4
3166			*16.7*	15.6
3266				15.9
3426				17.1
3626				18.4
3746				*20.1*

*(no cracking load retrieved)

However, comparing both test series and so only these two set of panels (Table 12 & Table 13) one can identify differences of the cracking loads up to 11.9 % and up to 9.5 % for the deflections (Slab12). The changes can be traced to the variations of the concrete or the bending stiffness of each slab, i.e. production tolerances as already noticed for the static deflections and dynamic parameters. Nevertheless, the cracking loads determined experimentally are in a good agreement with calculated values presented on Table 14. Also here with decreasing pretension force the cracking load is reduced.

Table 11. Difference of the cracking loads.

	Difference of the cracking load (experiment)			
Slab	Cracking load [kg]		Δ	Δ [%]
12	3746	3300	446	-11.9
11	3166	3200	34	+1.1
10	2986	2800	186	-6.2
9	1704-2556	2601	/	/

Table 12. Difference of the maximal deflection.

	Difference of the deflection (experiment)			
Slab	Deflection [mm]		Δ	Δ [%]
12	20.1	18.2	1.9	-9.5
11	16.7	16.5	0.2	-1.2
10	15.5	14.6	0.9	-5.8
9	8.5-15	13.6	/	/

Table 13. Cracking load of the two panels compared to the calculated cracking load.

	Cracking load [kg]		
Slab	calculated	Set 1	Set 2
12	3580	3300	3746
11	3350	3200	3166
10	3120	2800	2986
9	2890	2601	1704-2556

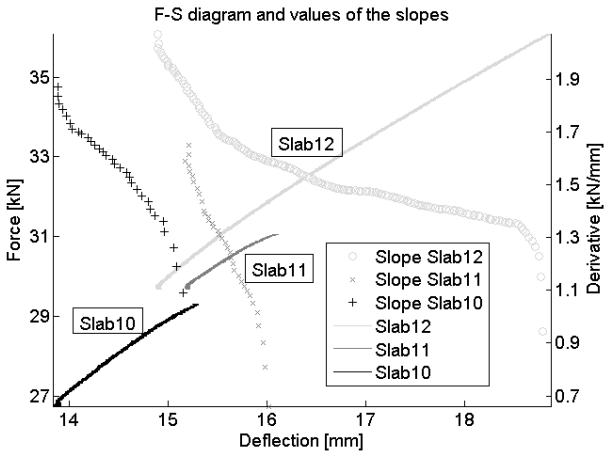

Figure 9. F-S diagram and calculated slopes A of the F-S curves for Slab10, Slab11 and Slab12.

Moreover for the last test series the deflection in the middle of each slab just before cracking are shown on Figure 9. In order to identify the slabs with reduced pretension force, the slopes of each F-S curve are numerically calculated. These are obtained using a rolling window, meaning that the slope of only 4000 data points (approximately 1500 N ≙ window size) is calculated. The gained slope value A (from the linear regression: y=Ax+B) is illustrated on the same figure as the F-S curves and represented by the symbols o, + and * for Slab12, Slab11 and Slab10 respectively. Then, the rolling window is shifted by 150 data points (55 N) and another slope value A is calculated and plotted. This is repeated until the appearance of the first crack. One can clearly recognise that the slope is flattened towards the end, illustrated by the drastically decreasing of A for each slab. Thus, one could say that by identifying these slopes and by looking simulatantanously to the deflection, non-destructive testing for a quality control could be possible, as the flattening of the F-S curves is a forward indication of crack formation and the deflection in function of the load an indicator on the pretension force.

4 CONCLUSION

The quality test of the prestressed slabs using dynamic and static testing methods is an interesting issue. As one can see on the presented evaluation for the unloaded and loaded states (smaller than the cracking load), the expecting values, meaning the highest deflection and the lowest frequency for the slab with three covered wires cannot be recognised. For the first test series the load on the slabs is too low and the influences of the bearing conditions too high to retrieve any information of reduced pretension. Further, the tolerances of the slabs, i.e. the bending stiffness of the concrete, are too big for this kind of tests to retreive any noticeable information. Therefore, small load testing demonstrates only concrete tolerances which preponderate over the changes due to the reduced pretension.

For the dynamic analysis, one sees for the second set of panels a clear dependency of the eigenfrequencies to the pretension force, but for the first set the right order of the eigenfrequencies according to the pretension force is not recognised leading to the conclusion that the test is not reproducible. Hence, the tolerances of the production are too big making dynamic parameters inapplicable to be used as a control on the pretension force.

However, the static and dynamic tests are in good correlation, as both methods identify the same order of stiffness for the two sets of panels.

Further, for the second and third test series the masses are increased to evaluate the cracking loads. These turn out to be a trustful indicator detecting the different pretension forces. In addition, a numerical differentiation could be used as a foreward indicator on the formation of cracks and, therefore, to manifest the cracking load before real cracking occurs. This concludes that such a non-destructive quality test could be possible, when evaluating the slope of the F-S diagram in real time in accordance with the deflection and the load.

5 ACKNOWLEDGEMENT

The authors would like to acknowledge ECHO for providing the special manufactured slabs.

6 REFERENCES

Mahowald, J., Bungard, V.; Maas, S.; Waldmann, D., Zuerbes, A. & De Roeck, G., 2010, Comparison of linear and nonlinear static and dynamic behaviour of prestressed and non-prestressed concrete slab elements, *Proceedings of The International Conference on Noise and Vibration Engineering – ISMA 2010*, Leuven, 2010, pp. 717-728

Ries, P., 2010, Analyse statischer und dynamischer Belastungsversuche zur Verbundprüfung bei Spannbetonhohldielen, *Bachelor Thesis, Université du Luxembourg, Faculté des Sciences, de la Technologie et de la Communication*, Luxembourg

Saiidi, M & Douglas, B. & Feng, S., 1994, *Prestress force effect on vibration frequency of concrete bridges, Journal of Structural Engineering*, Vol. 120, No. 7, pp. 2233-2241

Tibolt, A., 2011, Statische und dynamische Belastungsversuche zur Verbundprüfung bei Spannbetonhohldiehlen, *Bachelor Thesis, Université du Luxembourg, Faculté des Sciences, de la Technologie et de la Communication*, Luxembourg

Viera, J.S., 2010, Qualitätsprüfung einer Stahlbetonplatte mithilfe statischer und dynamischer Messmethoden, *Bachelor Thesis, Université du Luxembourg, Faculté des Sciences, de la Technologie et de la Communication*, Luxembourg

Waltering, M., 2009, Damage assessment of civil engineering structures and bridges using nonlinear dynamic characteristics, *PhD-Thesis, Université du Luxembourg, Faculté des Sciences, de la Technologie et de la Communication*, Luxembourg